



HAL
open science

Plastic biodegradation: Do *Galleria mellonella* Larvae Bioassimilate Polyethylene? A Spectral Histology Approach Using Isotopic Labeling and Infrared Microspectroscopy

Agnès Réjasse, Jehan Waeytens, Ariane Deniset-Besseau, Nicolas Crapart, Christina Nielsen-Leroux, Christophe Sandt

► To cite this version:

Agnès Réjasse, Jehan Waeytens, Ariane Deniset-Besseau, Nicolas Crapart, Christina Nielsen-Leroux, et al.. Plastic biodegradation: Do *Galleria mellonella* Larvae Bioassimilate Polyethylene? A Spectral Histology Approach Using Isotopic Labeling and Infrared Microspectroscopy. *Environmental Science and Technology*, 2022, 56 (1), pp.525-534. 10.1021/acs.est.1c03417 . hal-03544230

HAL Id: hal-03544230

<https://hal.inrae.fr/hal-03544230v1>

Submitted on 8 Dec 2023

HAL is a multi-disciplinary open access archive for the deposit and dissemination of scientific research documents, whether they are published or not. The documents may come from teaching and research institutions in France or abroad, or from public or private research centers.

L'archive ouverte pluridisciplinaire **HAL**, est destinée au dépôt et à la diffusion de documents scientifiques de niveau recherche, publiés ou non, émanant des établissements d'enseignement et de recherche français ou étrangers, des laboratoires publics ou privés.

1 Plastic biodegradation: Do *Galleria mellonella* Larvae Bioassimilate 2 Polyethylene? A Spectral Histology Approach Using Isotopic 3 Labeling and Infrared Microspectroscopy

4 Agnès Réjasse,* Jehan Waeytens, Ariane Deniset-Besseau, Nicolas Crapart, Christina Nielsen-Leroux,
5 and Christophe Sandt*



Cite This: <https://doi.org/10.1021/acs.est.1c03417>



Read Online

ACCESS |



Metrics & More



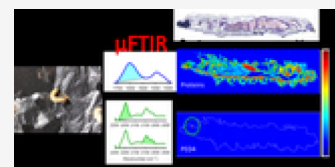
Article Recommendations



Supporting Information

6 **ABSTRACT:** Environmental pollution by the nearly nonbiodegradable polyethylene (PE)
7 plastics is of major concern; thus, organisms capable of biodegrading PE are required. The larvae
8 of the Greater Wax Moth, *Galleria mellonella* (Gm), were identified as a potential candidate to
9 digest PE. In this study, we tested whether PE was metabolized by Gm larvae and could be found
10 in their tissues. We examined the implication of the larval gut microbiota by using conventional
11 and axenic reared insects. First, our study showed that neither beeswax nor LDPE alone favor the
12 growth of young larvae. We then used Fourier transform infrared microspectroscopy (μ FTIR) to
13 detect deuterium in larvae fed with isotopically labeled food. Deuterated molecules were found in tissues of larvae fed with
14 deuterium labeled oil for 24 and 72 h, proving that μ FTIR can detect metabolization of 1 to 2 mg of deuterated food. Then, Gm
15 larvae were fed with deuterated PE (821 kDa). No bioassimilation was detected in the tissues of larvae that had ingested 1 to 5 mg of
16 deuterated PE in 72 h or in 19 days, but micrometer sized PE particles were found in the larval digestive tract cavities. We evidenced
17 weak biodegradation of 641 kDa PE films in contact for 24 h with the dissected gut of conventional larvae and in the PED4 particles
18 from excreted larval frass. Our study confirms that Gm larvae can biodegrade HDPE but cannot necessarily metabolize it.

19 **KEYWORDS:** polyethylene, plastic degradation, biodegradation, *Galleria mellonella* larvae, FTIR microspectroscopy, isotopic labeling,
20 hyperspectral imaging



21 ■ INTRODUCTION

22 Due to high production, inefficient waste collection and long
23 lifetime, plastics are now a major cause of environmental
24 pollution in land and maritime environments.¹ Development of
25 new biodegradable plastics and new plastic degradation
26 processes are pursued to remediate these problems. Biode-
27 gradation would offer advantages over other methods (landfill
28 storage, incineration, chemical degradation) as it can be more
29 environmentally friendly, produces less waste, and reduces the
30 cost of waste management. Polyethylene (PE), one of the most
31 produced plastics, is considered almost nonbiodegradable. PE
32 is synthesized in many forms with various molecular weights
33 (MW): PE wax (MW < 1000 Da), linear low-density PE
34 (LLDPE), low density PE (LDPE), and high density PE
35 (HDPE with MW of several millions of Da). They differ by
36 their molecular weights, chain lengths, degrees of branching,
37 packing densities, and crystallinities which affect biotic
38 degradation. Biodegradation is slower for PE with lower
39 branching, higher crystallinity, and chain lengths for HDPE.
40 Hydrophobic surface properties, glass transition temperature
41 (chain mobility), and long-range structure (surface area etc.)
42 may also affect biodegradation. Furthermore, to increase its
43 lifetime, PE is generally synthesized with antioxidants and UV
44 stabilizers.² Modest biodegradation rates were reported in the

literature by microorganisms from natural microbial communi-
ties.^{3–6}

Another potential plastic biodegradation method reported in
the literature is the use of insect larvae or their commensal gut
microorganisms.^{7–13} Several recent studies reported degrada-
tion of PE by the caterpillars of the Greater Wax Moth *Galleria*
mellonella (Gm).^{11,12,14–16} There is a rational motivation for
the use of these larvae. The metabolic pathways involved in the
degradation of long-chain hydrocarbons (like long-chain fatty
acids) are expected to play an important role in the
degradation of PE that is composed of a long aliphatic chain.
Since, Gm larva feeds on and metabolizes long-chain
hydrocarbons from beeswax,¹⁷ it may also potentially
metabolize PE. If this is the case, the role of gut enzymes
and the gut microbiota should be assessed. However, the
involvement of the larval gut microbiota may be questionable.
Recently, Kong et al.¹⁴ reported PE biodegradation independ-
ent of the intestinal microbiota while Ren,¹² Cassone,¹⁶ and

Received: May 27, 2021

Revised: November 26, 2021

Accepted: December 1, 2021

63 Lou¹⁸ described the implication of various species from the
64 Gm gut microbiota. In addition, the original study¹¹ reporting
65 the degradation of PE by the Gm larva was criticized on several
66 methodological points by Weber et al.¹⁹ Indeed, the approach
67 used to investigate the potential of the larvae to metabolize PE
68 in those studies presents several issues: gut residues on the PE
69 films are often misinterpreted for PE oxidation;²⁰ the ingestion
70 of PE does not imply metabolization of the polymer, and PE
71 metabolization by the larvae was never demonstrated. PE could
72 be biodegraded by gut bacteria and yet not be metabolized by
73 the larvae and not transformed into biological tissue. This and
74 the controversial results about microbiota involvement make it
75 necessary to further investigate whether Gm larvae and/or
76 their microbiota can really biodegrade and metabolize PE.

77 In this study, we present a methodology capable of detecting
78 the eventual metabolization of PE by Gm larvae. First, we
79 tested whether PE can be used as an energy source and if it
80 provided nutritional value for the Gm larvae. Then, we used
81 Fourier transform infrared microspectroscopy (μ FTIR) to
82 perform hyperspectral imaging of cryo-sections of the whole
83 larvae, and we evaluated the capability of Gm larvae to
84 bioassimilate PE as well as its integration in the larval tissues.
85 We developed an original protocol using polyethylene
86 isotopically labeled with deuterium (PED4) to detect if
87 deuterated molecules were metabolized in the Gm larval tissue
88 after deuterated PE ingestion. Indeed, based on its infrared
89 spectrum, the $-\text{CH}_2-$ peak from PE cannot be distinguished
90 from the $-\text{CH}_2-$ peak from lipids in larva tissues at low
91 concentrations, whereas $-\text{CD}_2-$ from deuterated PE has
92 specific absorption peaks in the infrared transparency window
93 of the tissues and could be easily identified in the larvae. The
94 large shift in peak positions between C–H and C–D is caused
95 by the larger atomic mass of deuterium causing a strong shift in
96 the vibration frequency of the C–D bonds. This method is one
97 of the most relevant to reveal metabolization. Furthermore,
98 PED4 and regular PE exhibit similar chemical and physical
99 properties, and their biodegradation products are expected to
100 be identical. After metabolization, PED4 should be found as
101 deuterated molecules containing $-\text{CD}_2-$ moieties, presumably
102 in tissues containing long aliphatic chains molecules.
103 Detecting $-\text{CD}_2-$ groups in the tissues of the larvae should
104 be a direct indication of PE metabolization. The sensitivity and
105 relevance of the method were evaluated by feeding experi-
106 ments with deuterated oil. The implication of the gut
107 microbiota in the biodegradation process was evaluated using
108 both conventional and axenically reared larvae (without
109 microbiota). The PE nutritional value was evaluated by
110 following larval growth with different diets at two development
111 stages.

112 ■ MATERIALS AND METHODS

113 **PE Materials.** Low density PE supermarket bags were used
114 for insect feeding and growth experiments. High density PE
115 bags were used for assessing the oxidation of PE in contact
116 with the dissected Gm larva gut. Perdeuterated PE flakes
117 (PED4) were purchased from Medical Isotopes Inc. (Pelham,
118 NH, U.S.A.). The crystallinities X_c of the PEs used in this study
119 were measured by FTIR spectroscopy using the method of
120 Hagemann²¹ and are described in the [Supporting Information](#).
121 We found a X_c of 0.83 for HDPE, a X_c of 0.68 for LDPE, and a
122 X_c of 0.91 for PED4. The PEs used in this study were
123 characterized by high-temperature gel permeation chromatog-
124 raphy (HT-GPC) by the Peakexpert company (Tours,

France). HT-GPC was performed at 150 °C in stabilized
trichlorobenzene on Agilent Mixed-B columns. Columns were
calibrated with polystyrene references. The average molecular
weights were found as follows: LDPE bags Mn 40.7 kDa, Mw
249.0 kDa, Mz 679 kDa; HDPE bags Mn 34.2 kDa, Mw 641.1
kDa, Mz 4277 kDa; PED4Mn 139.7 kDa, Mw 821.7 kDa, Mz
3354 kDa. All samples presented large MW distributions
ranging from hundreds to millions of Daltons. The molecular
weight distributions of the three PE samples (LDPE bags,
HDPE bags, and PED4) are shown in [Supplementary](#)
[Information \(Figure S6\)](#).

Insect Rearing and Feeding. Gm larvae were produced
on site in the insectarium at INRAE Micalis Institute at Jouy-
en-Josas, France. Gm eggs were hatched at 27 °C, and the
larvae were reared on beeswax and pollen (La Ruche
Roannaise, Roanne, France) with a 12 h day/12 h night
cycle in an MLR352H-PE Environmental Test Chamber
(Panasonic Healthcare Co, Ltd. Japan). The feeding assays
were performed in the dark.

The moths laid eggs on paper that were directly placed on
pollen and covered with beeswax in closed aerated plastic
boxes. For the axenic larvae, eggs were first sterilized by 10 min
of exposure on each side with UV light at 254 nm and fed with
gamma-ray sterilized pollen and beeswax in an autoclaved glass
jar with an aerated lid covered by sterile gauze and carded
cotton. The boxes and the jars were placed in an incubator at
27 °C, simulating the day–night cycle.

In order to verify that the larvae were axenic, 2 larvae were
crushed and homogenized with a sterilized pestle in 500 μL of
sterile physiological water, and 100 μL of the suspension were
spread on a BHI Petri dish. No bacterial growth was observed
after 7 days at 37 °C, and no bacterial 16S DNA was found
following V3/V4 PCR;²² for conventional larvae, 10⁶ bacteria/
larva were found.

Effect of Diet on Insect Growth. L2–L3 early stage larvae
(20 mg each) were placed individually in 12-well plates and
were either starved or fed *ad libitum* with one of five different
diets: beeswax alone, pollen alone, LDPE alone, beeswax +
pollen, or beeswax + LDPE. Six larvae were used for each diet
for a total of 36 larvae. The food uptake was evaluated by
weighing the remaining food. The larvae were kept at 27 °C
and weighed individually every 2–3 days. The test was
continued for 16 days until the larvae fed a beeswax + pollen
diet reached stage L6.

A second test was carried out with another batch of 36 L6-
larvae (last larval stage, 160 mg), 6 for each diet. The larvae
were placed individually in 6-well plates at 27 °C and fed with
LDPE as previously described. The larvae reached the chrysalis
stage in 8–10 days; the test was carried out for an additional
12 days until the adult stage.

The average growth of the 6 larvae and the standard
deviations were calculated with the “Origin Pro 2016” software
(Origin lab, Northampton, MA).

Perdeuterated Oil Feeding. Five conventional and five
axenic L6 stage larvae were starved for 24 h before free-feeding
for 24 or 72 h with pollen soaked with perdeuterated oil with a
density of 0.887 g/mL (*N*-hexadecane ($\text{C}_{16}\text{D}_{34}$, 98%),
Cambridge Isotope Laboratories, Inc., U.S.A.). Larvae fed for
24 h each ingested 6.7 mg of pollen and 1.6 μL (1.4 mg) of oil;
larvae fed for 72 h ingested each 20 mg of pollen and 4.8 μL
(4.2 mg) of oil.

Perdeuterated Polyethylene (PED4) Feeding. PED4
was received in flakes of several millimeters cubed. PED4 films

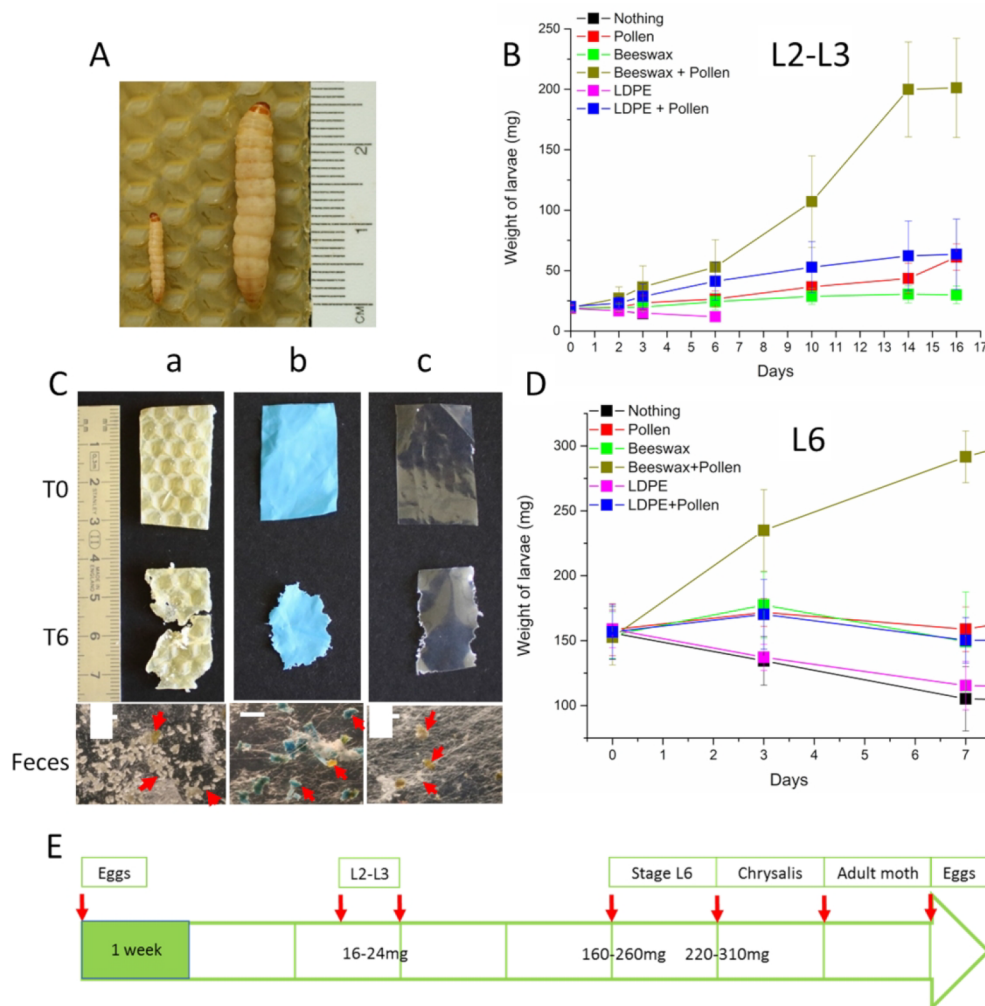


Figure 1. Evaluation of the nutritional value of different diets in Gm. (A) Gm larvae on beeswax: L2-L3 stage on the left, L6 stage on the right. (B) Growth curve of L2-L3 Gm larvae fed different diets. L2-L3 larvae ate 0.6 ± 0.3 and 2.5 ± 2.2 mg of LDPE per larva for the PE alone and PE + pollen diet, respectively. Larva fed PE alone died in 3 to 6 days. (C) Pictures evidencing the consumption of beeswax or LDPE at T0 and T6 (zero and 6 days) and the excretion of LDPE in feces. Arrows show the feces and PE fragments among the silk fibers. Scale bars: 2 mm. (D) Growth curve of last stage L6 Gm fed different diets. (E) Typical Gm larva evolution time scale (weeks) and larval weight (L2-L3 and L6) when fed with beeswax and pollen. Larvae were reared at 27°C .

188 were prepared either by pressing PED4 flakes at 140°C for
 189 15–30 min in an in-house designed press giving 30 to 40 μm
 190 thick films or by pressing PED4 flakes at room temperature for
 191 1 min at $15\text{ ton}/\text{cm}^2$ in a Specac manual hydraulic press
 192 (Eurolabo, Paris, France).

193 Two batches of L6 stage larvae (5 axenic and 5
 194 conventional) were starved for 24 h at 27°C in individual
 195 boxes. The larvae were then allowed to feed freely on PED4
 196 films for 3 days. The larvae were then killed by quick freezing
 197 and cryo-sectioned. The amount of PED4 ingested was
 198 evaluated by weighting the PED4 film left over, and feces
 199 were collected and stored at -80°C for further evaluation.
 200 Only larvae fed with more than 1 mg of PED4 were analyzed
 201 by μFTIR . Three axenic and three conventional larvae were fed
 202 for up to 19–21 days with PED4 alternating with pollen to
 203 allow survival.

204 **Cryo-sectioning and Preparation for Hyperspectral IR**
 205 **Imaging.** The cryo-sections were prepared on the Abridge
 206 platform (INRAE, Jouy-en-Josas, France). The larvae were
 207 frozen in a SnapFrost system (Excilone, Elancourt, France) in
 208 isopentane at -80°C and then stored at -80°C . The 10 and

20 μm sagittal sections were cut at -20°C with a Shandon 209
 FSE cryostat (ThermoFisher, Courtaboeuf, France). The 20
 210 μm thick sections improved the sensitivity of the detection for
 211 the weak C–D peaks, but tissue lipid and protein peaks were
 212 saturated. Consecutive sections were made and deposited on
 213 different slide supports: on StarFrost (Knittelglass, Germany) 214
 for immediate cresyl-violet staining, on SuperFrost plus
 215 (ThermoFisher, France) for histological staining, and on IR-
 216 grade polished IR-transparent CaF_2 slides (Crystran, Poole, 217
 U.K.) for IR hyperspectral imaging. The sections on CaF_2 were
 218 stored in a desiccator under a continuous flow of nitrogen until
 219 analysis. 220

221 **Hyperspectral FTIR Imaging.** Fourier transform infrared
 222 hyperspectral images were recorded at the SMIS beamline,
 223 SOLEIL synchrotron, France, on a Cary 620 infrared
 224 microscope (Agilent, Courtaboeuf, France) equipped with a
 225 128×128 pixel Lancer Focal Plane Array (FPA) detector and
 226 coupled to a Cary 670 spectrometer. Hyperspectral images
 227 were measured in transmission in the standard magnification
 228 mode with a $4\times/0.2$ NA Schwarzschild objective and matching
 229 condenser giving a field of view of $2640 \times 2640\ \mu\text{m}^2$ and a 229

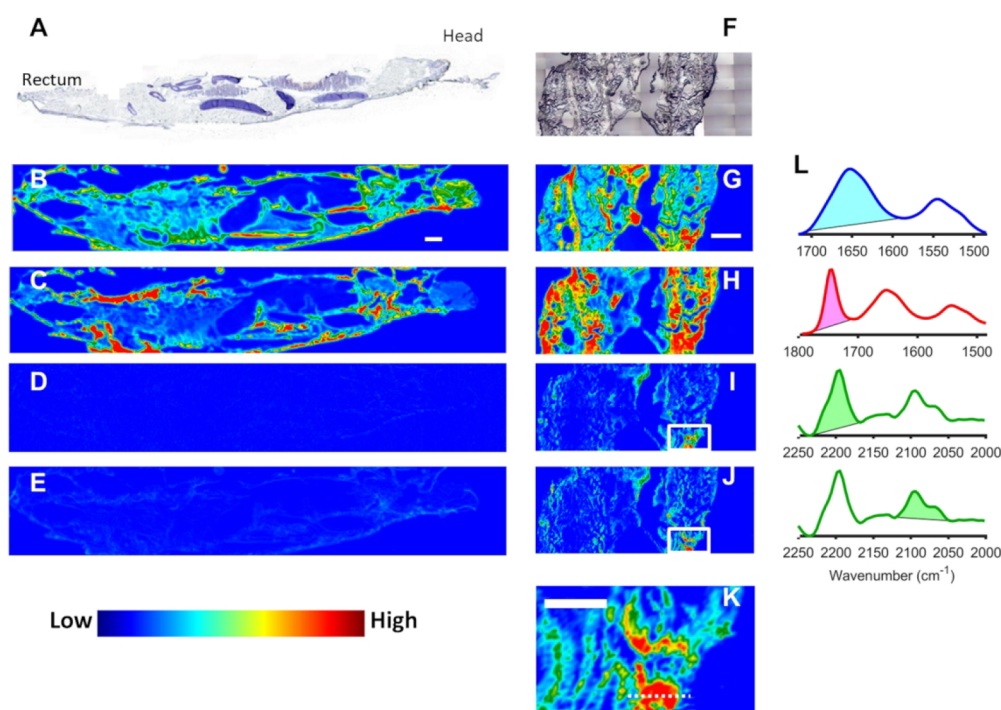


Figure 2. Spectral histology of Gm larvae and detection of C16D34 signal in larva sections. (A–E) Micrographs of a section of a control larva (4× magnification). (A) Bright field of cresyl violet stained section. (B–E) Infrared spectral histology maps showing the distribution of (B) proteins and (C) lipids; the absence of a C–D peak at (D) 2197 cm^{-1} and at (E) 2098 cm^{-1} . This shows that deuterium is not found in the control larva. (F–K) Micrographs of unstained larva fed for 72 h with C16D34 oil. (F) Bright field of the unstained section. (G–K) Infrared maps of (G) protein distribution and (H) lipid distribution. The detection of C–D peaks in the deuterated oil fed larvae is evidenced in (I) by the 2197 cm^{-1} C–D peak area from CD2 asymmetric stretching and in (J) by the 2098 cm^{-1} C–D peak area from CD2 symmetric stretching. (K) Zoom on a C–D-rich region delimited by the box in images I and J. Scale bars: 0.5 mm. (L) The peak area used for plotting the spectral maps, in descending order: protein amide I, lipid ester C=O, and symmetrical and asymmetrical C–D stretching peaks of the $\text{C}_{16}\text{D}_{34}$ oil.

230 projected pixel size of $20.4 \times 20.4 \mu\text{m}^2$. The actual spatial
231 resolution of the images was evaluated by the step-edge
232 method to be approximately $40 \mu\text{m}$ at 1545 cm^{-1} and $30 \mu\text{m}$ at
233 2915 cm^{-1} . Mosaics composed of several FPA tiles were
234 recorded to image the whole sections.

235 Hyperspectral images were recorded between 900 and 3900
236 cm^{-1} at 8 cm^{-1} resolution, with 256 and 128 co-added scans
237 for background and sample, respectively.

238 **Synchrotron Radiation FTIR Microspectroscopy (SR-
239 μFTIR).** SR- μFTIR was performed at the SOLEIL synchrotron
240 facility on the SMIS beamline.²³ The synchrotron was operated
241 at 500 mA in top-up mode for injections. Spectra and maps of
242 the sections were recorded using Continuum microscopes
243 coupled to Nicolet 8700 or 5700 spectrometer (ThermoFisher,
244 Courtaboeuf, France). The microscopes were equipped with
245 $32\times/0.65$ NA Schwarzschild objectives and matching con-
246 densers and liquid-cooled narrow-band MCT/A detectors.
247 The confocal aperture was set at $12 \times 12 \mu\text{m}^2$. Spectra were
248 recorded in transmission mode at 6 cm^{-1} resolution with 16 to
249 32 scans between 650 and 4000 cm^{-1} .

250 **Data Analysis.** Spectral images were computed in
251 ResolutionPro (Agilent) and in Quasar.^{24,25} Spectral images
252 were created using the baseline-corrected, integrated areas of
253 the peaks of interest. Lipid and protein distributions were
254 imaged by the C–H stretching peaks of CH_2 and CH_3
255 between 2800 and 3000 cm^{-1} and the amide I band between
256 1590 and 1705 cm^{-1} , respectively. The deuterated PE was
257 detected and imaged by symmetric and asymmetric CD₂
258 stretching peaks at 2085 cm^{-1} (2030 – 2130 cm^{-1}) and 2190
259 cm^{-1} (2165 – 2230 cm^{-1}). The deuterium/protein peak area

ratio was computed with protein band area integrated between 260
1480 and 1720 cm^{-1} . K-means clustering of the hyperspectral 261
images and computation of Pearson correlation coefficients 262
between peak-area ratios were performed in Quasar. K-means 263
clustering is a multivariate pattern-recognition method that 264
allows clustering spectra based on their similarities; 10 runs 265
and 300 iterations were used. Water vapor subtraction was 266
performed in Matlab 2016 (MathWorks, Natick, MA) with an 267
in-house script. 268

269 ■ RESULTS

270 **Nutritional Value of PE.** To estimate the relative 270
nutritional value of PE as an energy source for Gm, we 271
compared the food uptake, weight gain, and larval survival for 272
different diets: control (nothing), pollen alone, beeswax alone, 273
beeswax + pollen, LDPE alone, and LDPE + pollen. We set up 274
growth experiments with conventional larvae at two different 275
stages (Figure 1A,E): young larvae (L2–L3 stage, 20 mg per 276
larva) and last instar (L6 stage, 160 mg). 277

278 For L2–L3 larvae (Figure 1B), the nibbling of PE was 278
difficult to observe and LDPE consumption was estimated by 279
weighing the remaining PE (Supporting Information Table 1). 280
The larval weight uptake was followed up to 16 days. The 281
weight of larvae fed with a pollen–beeswax diet increased 10 282
times, while with a pollen-only diet, it increased 3 times and 283
1.3 times with a beeswax-only diet. The pollen–beeswax diet 284
was the optimal condition for Gm larval growth. The control 285
larvae, without food, died after 3 days. Larvae fed with only 286
LDPE lost weight (1.3-fold), did not change growth stage, and 287
exhibited 50% mortality at day 3 and 100% mortality at day 6, 288

289 probably due to starvation. Larvae fed with both LDPE and
290 pollen did not gain weight compared to larvae fed only with
291 pollen. This indicated that although they consumed LDPE
292 (Figure 1B), it did not provide energy for growth or survival at
293 early development stages (see detailed diet consumption in
294 Supporting Information Table 1).

295 For L6 larvae, LDPE consumption was observed directly on
296 colored and not-colored commercial LDPE films. Residues of
297 colored PE were found in the excreted feces (Figure 1C). We
298 followed the growth of L6 stage larvae fed with different diets
299 for 7 days (Figure 1D and Supporting Information Table 2).
300 The results demonstrate that—as for the young larvae—the
301 best diet was a combination of beeswax and pollen, since the
302 larvae almost doubled weight in 7 days. Larvae fed with a
303 pollen-only diet, wax-only diet, or LDPE–pollen diet survived
304 but did not gain weight. Larvae fed with LDPE-only diet lost
305 25% of their weight as did the control larvae (no food), but all
306 survived and were able to complete metamorphosis into a
307 moth, like in all the other conditions. In average, larvae fed
308 with a pollen–PE diet had each consumed 0.48 mg PE/day/
309 larva, and larvae fed with a PE-only diet consumed 0.37 mg
310 PE/day/larva; these rates are comparable to those reported by
311 Lou¹⁸ (0.60 mg PE/day/larva) but inferior to those reported
312 by Bombelli¹¹ (1.84 mg PE/day/larva).

313 These experiments show that conventional Gm larvae ingest
314 PE but cannot derive nutritional value from it.

315 **Hyperspectral Infrared Imaging of Larva Cryo-**
316 **sections.** Although the larvae did not gain weight by eating
317 PE in the aforementioned experiment, it does not prove that
318 Gm larvae or their microbiota could not metabolize small
319 quantities of this PE. Therefore, we developed a method based
320 on μ FTIR^{26,27} hyperspectral imaging for measuring the
321 chemical composition of the Gm larvae tissues. The ultimate
322 goal was to detect the presence of metabolized PE in the tissue
323 following ingestion of deuterated PE.

324 First, we set up the μ FTIR hyperspectral imaging experiment
325 to measure the spectral tissue composition (sugars, proteins,
326 and lipids) and if deuterium can be detected in Gm larvae thin
327 sections in larvae fed with an optimal pollen and wax diet.
328 Hyperspectral infrared images of 10 μ m thick cryo-sections of
329 control larvae were recorded (Figure 2A–E). The spectra and
330 peak area used to generate the spectral maps are shown in
331 Figure 2L and Supplementary Figure S1. Representative
332 spectra from different tissues were obtained by classifying all
333 the larval tissue spectra in 4 groups by k-means clustering
334 (Supporting Information Figure S1A). The IR absorption
335 spectra from the larval tissues were typical biological tissue
336 spectra.²⁸ They were dominated by the absorption bands of the
337 stretching vibration of O–H and N–H bonds present in sugars
338 and proteins at 3400 and 3300 cm^{-1} ; C–H peaks from lipids
339 and proteins between 3020 and 2800 cm^{-1} ; C=O peaks from
340 esterified lipids at 1740 cm^{-1} and carboxylic acids at 1710
341 cm^{-1} ; CONH peaks from proteins at 1654 and 1545 cm^{-1} ; C–
342 H and COOH peaks between 1480 and 1350 cm^{-1} ; P=O
343 peaks at 1240 and 1080 cm^{-1} ; and C–OH, C–OP, COC, and
344 COH peaks from carbohydrates and lipids at 1160, 1150,
345 1100, 1035, and 1025 cm^{-1} . While proteins peaks are generally
346 the most intense peaks in the spectra of most animal tissues,
347 peaks from phospholipids and esterified lipids (C–H, C=O,
348 C–OC, and C–OP) strongly dominated the spectra of larva
349 tissues showing their extremely high lipid concentration. The
350 C=C–H olefinic peak from unsaturated lipids at 3008 cm^{-1}
351 was detected in the lipid-rich tissues, evidencing a strong lipid

unsaturation level. In Figure 2B,C, we present respectively the
352 protein and lipid distribution from the control larva section
353 shown in Figure 2A. Silk glands and some epithelial regions
354 (evidenced by the amide I band at 1650 cm^{-1}) appeared, like a
355 red hotspot in the protein image, while fatty tissues (evidenced
356 by esterified lipids by the ester C=O peak at 1740 cm^{-1})
357 appeared red in the lipid image. 358

No deuterium could be detected in control larvae by looking
359 at the 2000–2200 cm^{-1} range that contains the strongest C–D
360 stretching peaks. Figure 2D,E shows hyperspectral maps of the
361 larva cryo-section at 2197 and 2098 cm^{-1} , respectively, 362
evidencing the absence of detectable C–D peaks in the
363 control larvae. The faint tissue contours observed in Figure 2E
364 arise from baseline drifts caused by IR radiation scattering at
365 the edge of the tissue and not from the C–D peak. The typical
366 C–D peaks are shown in Supporting Information Figure S1B
367 in the spectrum of deuterated PED4 (red) and of deuterated
368 oil (green) dominated by the C–D stretching peak at 2197
369 and 2098 cm^{-1} , shown along with the spectrum of a normal PE
370 film (blue) dominated by the methylene (–CH₂–) peaks at
371 2914 and 2848 cm^{-1} . This shows that deuterium at natural
372 abundance is not detectable even in the fatty larval tissue since
373 natural concentrations are in the parts per million range,²⁹ well
374 below the detection limits of μ FTIR. 375

376 **Detection of Deuterium in Cryo-sections of Larva Fed**
377 **with Deuterated Oil.** In order to prove that deuterium could
378 be detected (as C–D bonds) in larvae that had ingested
379 deuterated food, conventional and axenic larvae were fed
380 during 24 and 72 h with C₁₆D₃₄ perdeuterated oil. The oil was
381 mixed with pollen to facilitate its ingestion since larvae would
382 not ingest pure oil. On average each larva had ingested 1.4 mg
383 of oil in 24 h and 4.2 mg in 72 h. The larvae were then cryo-
384 sectioned, and the thin sections were investigated by μ FTIR
385 (Figure 2F–K). A weak C–D signal could be detected after 24
386 h, at discrete locations (not shown), but the C–D signal was
387 consistently detected in most tissues after 72 h of feeding
388 (Figure 2I,J). This suggests that the threshold for consistent
389 detection was around 2 to 2.5 mg of ingested deuterated food.
390 The C–D signal was detected at discrete locations throughout
391 the sections and appeared stronger in some lipid rich tissues.
392 The related spectra can be seen in Supporting Information
393 Figure S1C showing the pure C₁₆D₃₄ oil spectrum and the
394 spectra from the different larval tissues. We found a moderately
395 positive correlation between the distribution of lipids and
396 deuterated molecules with a correlation coefficient of 0.42
397 between the C–D and C–H signals. This confirmed that
398 deuterated food assimilation could be detected more
399 sensitively in the fat tissues. Figure 2K shows a zoom on a
400 C–D-rich region, and the spectra are shown in Supporting
401 Information Figure S1D. The C–D signal measured with the
402 μ FTIR imaging system was low, with a maximum of 0.025 a.u.
403 at 2197 cm^{-1} in the hot spot shown in Figure 2K. We used a
404 confocal microscope coupled to a synchrotron source to
405 improve measurement sensitivity and accuracy (Figure S1E)
406 and measured a one order of magnitude higher C–D signal
407 (up to 0.20 A.U.) than with the imaging system. The
408 synchrotron data were then used to examine if the oil was
409 changed upon metabolism: the CD₂ peak position
410 (sensitive to the molecule environment) and the CD₂/CD₃
411 ratio (related to the aliphatic chain length) were determined
412 and compared in the pure oil and in the deuterated fatty
413 tissues. The CD₂/CD₃ ratio measured at 24 different positions
414 in the larval tissue varied between 0.72 and 3.6 (mean 2.16) 414

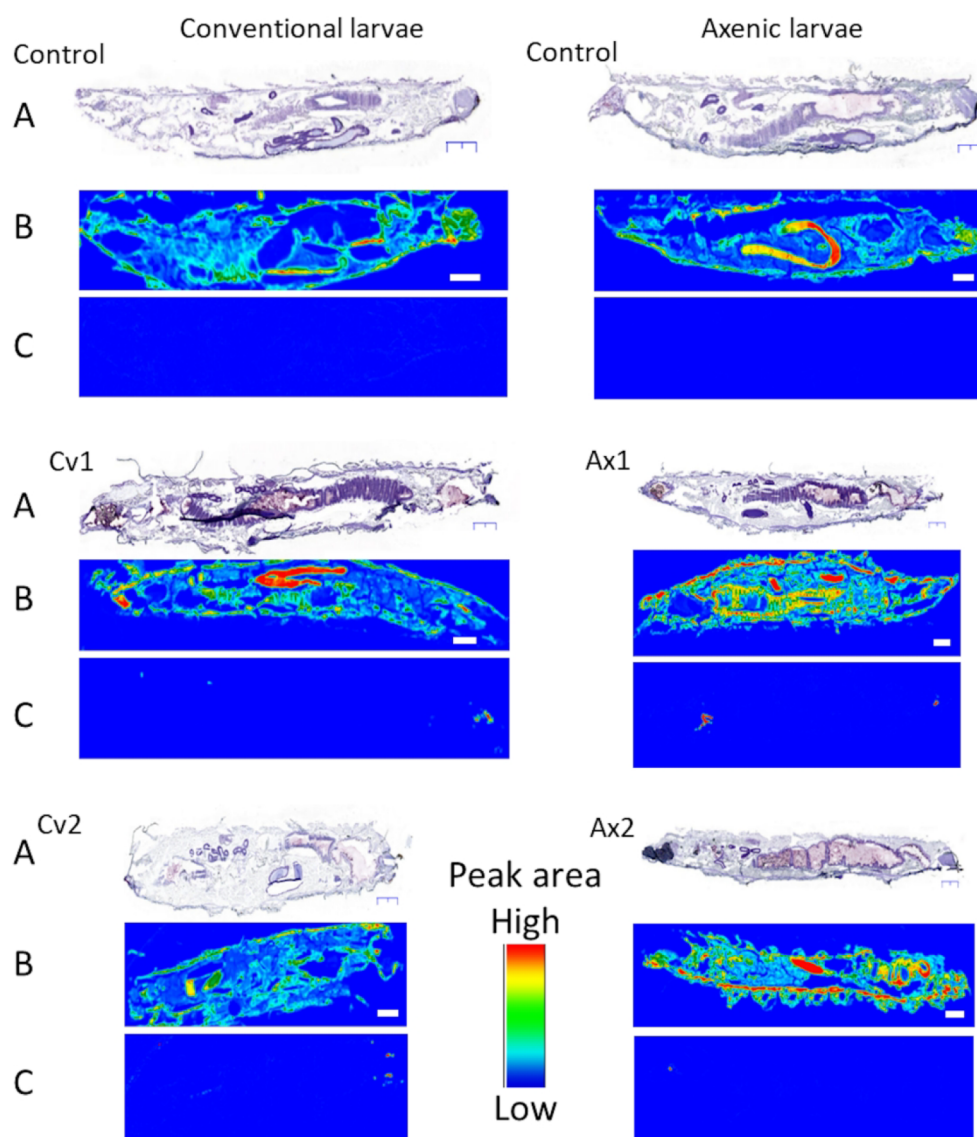


Figure 3. Presence of the C–D signal in Gm larvae fed with PED4. Conventional (Cv) and axenic (Ax) control larvae were fed with nondeuterated PE for 3 days, and test larvae were fed with deuterated PE for 3 days (Cv1 and Ax1). Cv2 and Ax2 larvae were fed with alternating diets (see [Materials and Methods](#)) over a period of 19 days. Sections were stained with cresyl violet and observed in bright field microscopy (A) or kept unstained and analyzed by μ FTIR (B and C). The IR hyperspectral images show the distribution of (B) proteins (1650 cm^{-1} amide I peak area) and (C) deuterated PE (2197 cm^{-1} C–D peak area). No deuterated molecules were found in the tissue of the conventional and axenic control larvae or in the Cv1, Ax1, Cv2, and Ax2 larvae, but few deuterated PE particles were detected in the mouth, gut, and rectum of both Cv and Ax larvae. Spectra from such particles are shown in [Figure S1F](#). Scale bar: 1 mm and magnification was $4\times$ in both IR and visible micrographs.

415 and was different from its value in the pure oil (1.92) showing
416 that the oil was fragmented and CD_2 moieties were integrated
417 in shorter and in longer aliphatic chains. This supported the
418 idea of metabolism of the oil in the larva. The CD_2 peak
419 positions in pure oil and in the tissues were not significantly
420 different at $2197.1 \pm 1.2\text{ cm}^{-1}$ and $2197.3 \pm 0.4\text{ cm}^{-1}$,
421 respectively (student $p > 0.05$). The positions of the C–D
422 peaks are sensitive to the conformation of lipids to their local
423 environment and to the long-range order such as the
424 organization in amorphous gel or liquid crystal.³⁰ This showed
425 that the deuterated lipids were in similar environments in the
426 pure oil and in the tissues, probably as small droplets, and that
427 the differences in CD_2/CD_3 ratio were not due to local
428 environment changes.
429 These results clearly demonstrate that the larvae were able
430 to metabolize and integrate deuterated food into their fatty

tissue and that μ FTIR hyperspectral imaging is sensitive 431
enough to detect the metabolism of a few milligrams of 432
deuterated food. 433

**Investigations into Cryo-sections of Larva Fed with 434
Deuterated PE.** Therefore, we then investigated whether Gm 435
larvae fed with deuterated PE (PED4) were able to assimilate 436
PE by seeking the appearance of C–D peaks in the larval 437
tissues. Similarly, we recorded hyperspectral infrared images 438
from sections from 5 conventional and 5 axenic L6 larvae fed 439
for 3 days with PED4 and 2 conventional and 2 axenic control 440
larvae fed with nondeuterated PE. For each larva, two cryo- 441
sections, one $10\text{ }\mu\text{m}$ thick and one $20\text{ }\mu\text{m}$ thick, were analyzed. 442
Each larva ingested on average 2.1 mg of PED4 (min 1 mg, 443
max 4 mg) or 0.7 mg of PED4/day/larva for L6 larvae. This 444
rate is similar to that of normal LDPE and to those reported in 445
the literature by Lou et al.¹⁸ Three additional L3 larvae were 446

fed for 19 days with PED4 alternating with a pollen diet to keep them alive and ate 3.6 mg of PED4 on average. This was comparable to the quantities of deuterated oil ingested by the larvae (1.4 mg and 4.2 mg at 24 and 72 h, respectively).

The results are presented in Figure 3, which shows visible and IR hyperspectral images of one representative larval cryo-section for each condition. IR hyperspectral images of the protein peak at 1650 cm^{-1} and CD_2 peak at 2197 cm^{-1} are shown. In the control axenic and conventional larvae, no absorption of C–D could be detected in the tissues, as expected. No C–D peak was detected in the tissues of the 5 conventional and 5 axenic larvae fed for 3 days with PED4. To ensure that it was not due to a sensitivity issue, 20 μm thick sections were studied, giving the same results. In order to further boost the sensitivity of the method, another set of conventional and axenic L3 stage larvae were fed during 12 to 19 days with PED4. To make sure that the larvae could survive over 6 days with this low nutritional value diet, the 12- and 19-days periods were fractioned in periods of 3 days alternating between the PED4-only diet and PED4 plus pollen diet. These L3 larvae had consumed 3.6 ± 1.1 mg PED4 per larva at the end of the experiment at rates of 0.19 to 0.28 mg PED4/day/larva (L3 larvae eat less than L6 larvae).

No C–D peak was detected in the tissues of these L3 larvae (Cv2 and Ax2 in Figure 3).

However, particles with a C–D signal were detected in cavities of the digestive tract such as the mouth, the gut, and the rectum in 6 out of 10 of the conventional and axenic larvae fed with PED4. This corresponded to the presence of micrometer sized PED4 particles (25–50 μm) and aggregates (up to 1000 μm). The larger PED4 particles were observed in the oral cavity and rectum. No differences were observed between axenic and conventional larvae. The particles appeared more numerous in the mouth and rectum, and fewer particles were found in the gut. Since no embedding was used, it is possible that some of the gut particles were lost during sectioning. While the largest particles could be detected by microscopic observation, the C–D IR signature allowed detecting smaller particles. The spectral signature also allowed confirming the chemical nature of the particles. To investigate whether smaller particles present in the gut could escape detection with hyperspectral imaging, we also recorded SR- μFTIR maps and were able to detect micrometer-sized PE particles in the gut of the larvae (Figure S1F). We also tried to evaluate whether the PED4 found in the digestive tract was oxidized by analyzing the CD_2/CD_3 ratio of the gut particles using the SR- μFTIR data. However, most particles were either too thick or too scattered to yield good quality spectra that could be used for such analysis.

Biodegradation of PE by Gm Larvae. The absence of PE bioassimilation could be due to an inability of our Gm larva population to biodegrade PE. We investigated this ability by using two methods: detection of PE oxidation by μFTIR imaging of HDPE films in contact with the dissected guts of Gm larvae and analysis of the CD_2/CD_3 ratio of PED4 particles in the Gm larval frass by ATR-FTIR. The results are detailed in the Supporting Information.

Weak PE oxidation was detected in the PE films in contact with the guts of conventional Gm larvae (Figure S2) by μFTIR imaging but not with guts from the axenic larvae. Meanwhile the results did not allow us to make a conclusion on the implication of the Gm microbiota since variations were found among the replicates of axenic larvae.

The CD_2/CD_3 ratio of PED4 particles in the gut of the larvae was measured by ATR-FTIR in the excreted larval frass (Supporting Information). It was found to be 15% lower for the PED4 particles in the frass (2.91 ± 0.32) than for the pristine PED4 films (3.42 ± 0.40), suggesting shorter aliphatic chains in the digested PED4, thus indicating some chemical modification and biodegradation of PED4 (Figure S3) in the gut.

DISCUSSION

The capability of Gm larvae to digest and bioassimilate PE is controversial^{11,12,14,16,19,31} and necessitates further investigation. The role of the Gm microbiota is also disputed.^{12,14,18} We therefore examined whether the Gm larvae with and without microbiota were only chewing PE or were truly able to digest and metabolize it.

Feeding experiments showed that pollen+beeswax was the optimal diet, in agreement with literature.^{14,17} Early larval stages L2–L3 fed with PE lost weight and died in 3 days (50%) to 10 days (100%). This trend is similar to results from Lou et al. (50% death at 15 days).¹⁸ Kong et al. reported 100% survival but 20–30% weight loss in PE-fed Gm larvae in 14 days.¹⁴ Billen et al. reported that an LDPE diet was not sufficient for sustaining Gm larva growth.³¹ Lemoine et al. reported a 50% weight loss on a PE diet.³² Our results suggested that a pollen-only diet is sufficient for the survival of the larvae and that an additional source of carbon such as beeswax allows larvae to gain weight, in agreement with the literature.^{17,14} L2–L3 larvae fed with pollen and PE survived 16 days and gained some weight but far less than the larvae fed with the optimal diet.

This trend was confirmed with the last stage (L6) larvae fed only with PE as they lost weight compared to larvae fed with pollen or beeswax and consumed 80 times less food than larvae fed with beeswax. We did not observe significant differences in feeding behavior or weight gain between conventional and axenic larvae, suggesting that the microbiota may not be important for their development and life cycle under our conditions and those reported by Kong.¹⁴ For L6 larvae, the final life cycle was similar for Gm larvae fed with PE or beeswax: after 8 days the larvae pupated, the adult moths appeared 1 week later, and egg production was similar. These experiments showed that PE does not have nutritional value for the Gm larvae. Larvae at the early L6 stage have accumulated enough reserves to continue their life cycle even if their diet is changed to PE alone, whereas larvae at an early stage cannot survive with PE alone.

We then evaluated whether PE could be bioassimilated by Gm larva. We developed a new approach based on the μFTIR hyperspectral imaging of carbon–deuterium bonds in cryo-sections of larvae fed with deuterated PE. This method could, potentially, not only allow showing the metabolization of PE but also help find in which tissues PE metabolites accumulate and what kind of biomolecules might be synthesized using PE. We first established that it was possible to detect the metabolization of deuterated food in the tissues of larvae fed with perdeuterated oil mixed with pollen: the C–D signal was indeed detected in most tissues and predominantly in fatty tissues (adipocytes) after a 3 day diet in both axenic and conventional larvae. The CD_2/CD_3 peak area ratio was modified compared to the original oil signal showing that the oil was integrated in shorter and in longer aliphatic chains. This demonstrated that μFTIR could detect the C–D signal in

572 tissue sections from larvae that had ingested and metabolized 1
573 to 4 mg of deuterated food.

574 On the contrary, we could not detect any C–D signal in L6
575 larvae fed with PED4 during 3 days or during 19 days. The
576 absence of the C–D signal indicated that the PE was not
577 metabolized and integrated in the larvae body in substantial
578 quantities. This should not be due to a lack of sensitivity of the
579 spectroscopic method since the larvae had ingested 2.1 mg of
580 PED4 per larva after 3 days and 3.6 mg of PED4 per larva after
581 19 days (up to 5 mg), while as discussed above a C–D signal
582 was consistently detected in most tissues when larvae ingested
583 4.2 mg of deuterated oil. We estimate that the method will
584 allow detecting reliably the assimilation of around 2 mg of
585 deuterated food and even lower quantities with the help of a
586 synchrotron source. Meanwhile, PED4 microparticles were
587 detected in the mouth, gut, and rectum of the larvae,
588 confirming that Gm larvae were able to break and masticate
589 the PE films in smaller, micrometer-sized particles. Instead of
590 metabolizing the plastic, the larvae generated micrometer-sized
591 particles which could be worse for the environment and more
592 difficult to collect than larger pieces of plastic.³¹

593 Polymer characteristics such as molecular weight, crystal-
594 linity, surface hydrophobicity, glass transition temperature, etc.
595 may hamper enzymatic biodegradation. The PED4 used here
596 had a higher average molecular weight (MW) of 821 kDa than
597 the HDPE and LDPE from commercial bags (641 kDa and
598 249 kDa, respectively). However, all 3 samples presented
599 broad MW distributions ranging from hundreds to millions of
600 Da (Supporting Information Figure S5). HDPE presented a
601 light chain fraction at 150 kDa and a heavy chain fraction at
602 300 kDa, and the PED4 had a MW distribution similar to this
603 heavier chain fraction and also centered at 300 kDa. PED4
604 crystallinity (0.9) also fell in the range of commercially
605 available HDPE (0.6–0.9). Thus, the PED4 used in this study
606 can be considered representative of the heavy fraction of
607 commercially available HDPE bags. Since plastic digestibility
608 may strongly depend on PE density, the next steps could be to
609 investigate the bioassimilation of deuterated LDPE with lighter
610 molecular weights, which could theoretically show better
611 bioassimilation.

612 Yang et al.³³ observed negligible integration of ¹³C in the
613 body of the beetle larvae of *Tenebrio molitor* Linnaeus fed with
614 ¹³C polystyrene (PS) and found that a large fraction of the ¹³C
615 was integrated in the CO₂ produced by the gut bacteria.
616 Recently, independent results of Cassone et al.¹⁶ and Ren et
617 al.¹² reported that bacteria isolated from the Gm larva gut were
618 able to grow on and degrade PE into smaller compounds,
619 implicating a role of the gut microbiota. Our results showed no
620 PE bioassimilation in either axenic or conventional larvae.
621 Since our Gm population was able to survive on beeswax,
622 develop on beeswax–pollen, and assimilate perdeuterated oil,
623 it does possess the required enzymes to efficiently metabolize
624 long- and short-length hydrocarbons. The absence of
625 bioassimilation even in conventional larvae with an intact
626 microbiota might indicate that our Gm population lacked some
627 of the bacterial species/strains capable of degrading PE in
628 smaller hydrocarbons that were present in other Gm
629 populations described in the literature. However, we found
630 weak oxidation in PE films in contact for 24 h with the
631 dissected gut of conventional larvae and a shortening of
632 aliphatic chains in PED4 particles excreted in the larval frass,
633 indicating that a PE oxidation capability exists in our Gm. The
634 oxidation of PE in the larval gut could favor its biodegradation

even in the absence of bioassimilation since oxidation is the 635
first step of environmental biodegradation. Several groups 636
reported isolating bacterial and fungal strains capable of 637
digesting PE from different Gm populations: Cassone reported 638
isolating an *Acinetobacter* sp. from Gm,¹⁶ while Ren reported 639
isolating an *Enterobacter* sp.,¹² and Zhang reported isolating an 640
Aspergillus flavus strain.³⁴ Yang isolated strains of *Bacillus* sp. 641
and *Enterobacter* sp. able to digest PE from the Gm related *P.* 642
interpunctella larvae.³⁵ The microbiota of our Gm population 643
was analyzed by 16S rRNA gene sequencing and was shown to 644
be composed of mainly Firmicutes (*Enterococcus*) and a lower 645
amount of Cyanobacteria and Proteobacteria, (Supporting 646
Information Figure S4). The Proteobacteria were mostly 647
Enterobacteriaceae, although *Acinetobacter* sp. was absent, and 648
the amount of proteobacteria was low. The *Enterococcus* 649
species in our Gm population suggested that its microbiota was 650
not fundamentally different from those reported by other 651
groups.¹⁸ In microbial biodegradation studies, most of the 652
identified bacteria belong to the Proteobacteria (48%) and 653
Firmicutes (37.4%),³⁶ which are also present in our Gm 654
microbiota. We will investigate the PE-degrading capacity of 655
the Gm microbiota. FTIR microspectroscopy could be used to 656
measure the integration of C–D in microcolonies of bacteria 657
grown on PED4 films and will be tested in our follow-up work. 658

■ ASSOCIATED CONTENT

SI Supporting Information

The Supporting Information is available free of charge at 661
<https://pubs.acs.org/doi/10.1021/acs.est.1c03417>. 662

Average food consumptions by L3 stage larvae (average 663
consumed weight per individual larva for 16 days); 664
average food consumptions by L6 stage larvae (average 665
consumed weight per individual larva for 7 days); 666
infrared spectra of the larval tissues, of normal 667
polyethylene and deuterated polyethylene, as film or as 668
particles found in the gut of larvae, and of the deuterated 669
oil used in this study in pure form and as found in the 670
larval tissues; results of the biodegradation of HDPE 671
films by the dissected gut of Gm larvae; evaluation of PE 672
oxidation after contact for 24 h with the guts of Gm 673
larvae; alteration of PED4 in the gut of the Gm larvae 674
evaluated by a change in the CD2/CD3 ratio directly in 675
the spectra of Gm larvae feces; analysis of Gm larva 676
microbiota by 16S rRNA sequencing; evaluation of the 677
crystallinity index of the various PE used in this study by 678
IR spectroscopy; and molecular weight distributions of 679
the PE used in this study (PDF) 680

■ AUTHOR INFORMATION

Corresponding Authors

Agnès Réjasse – *Université Paris-Saclay, INRAE,*
AgroParisTech, Micalis Institute, 78350 Jouy-en-Josas,
France; Email: agnes.rejasse@inrae.fr 683
684
685

Christophe Sandt – *SMIS beamline, Synchrotron Soleil,*
L'Orme des Merisiers, 91192 Cedex Gif-sur-Yvette, France;
orcid.org/0000-0002-6432-2004; *Email: sandt@*
synchrotron-soleil.fr 686
687
688
689

Authors

Jehan Waeytens – *Structure et Fonction des Membranes* 691
Biologiques, Université libre de Bruxelles, B-1050 Bruxelles, 692

693 Belgique; Université Paris-Saclay, CNRS, Institut de Chimie
694 Physique, UMR 8000, 91405 Orsay, France
695 Ariane Deniset-Besseau – Université Paris-Saclay, CNRS,
696 Institut de Chimie Physique, UMR 8000, 91405 Orsay,
697 France
698 Nicolas Crapart – UMR 1313 GABI, Abridge, INRAE,
699 Université Paris-Saclay, 78350 Jouy en Josas, France;
700 Exilone, 78990 Elancourt, France
701 Christina Nielsen-Leroux – Université Paris-Saclay, INRAE,
702 AgroParisTech, Micalis Institute, 78350 Jouy-en-Josas, France

703 Complete contact information is available at:
704 <https://pubs.acs.org/10.1021/acs.est.1c03417>

705 Author Contributions

706 A.R. initiated the study, designed the research, reared the
707 insects, performed insect feeding experiments, and participated
708 in the writing of the manuscript. J.W. performed infrared
709 microspectroscopy measurements, prepared figures, and
710 participated in the writing of the manuscript. A.D.-B.
711 participated in the study design and corrected the manuscript.
712 N.C. performed insect cryo-section and tissue coloration. C.N.-
713 L. participated in the study design and corrected the
714 manuscript. C.S. designed the infrared microspectroscopy
715 study, performed the infrared microspectroscopy measure-
716 ments, prepared figures, and wrote the manuscript.

717 Notes

718 The authors declare no competing financial interest.

719 ACKNOWLEDGMENTS

720 The authors acknowledge the Synchrotron SOLEIL for
721 provision of synchrotron radiation facilities and FTIR
722 microspectroscopy equipment. The authors also acknowledge
723 the INRAE-Jouy-en-Josas histology platform (Abridge) for the
724 cryo-sectioning and microscopy facilities and the INRAE-
725 MICA department for the general support to C.N.-L. and A.R.
726 The authors acknowledge Stéphane Chaillou from INRAE-
727 MICALIS team FME for deciphering the Gm microbiota using
728 16SRNA gene sequencing and for useful discussion. The
729 authors wish to acknowledge DIM-ACAV from Région Ile de
730 France for financial support.

731 ABBREVIATIONS

732 Gm, *Galleria mellonella*; PE, polyethylene; LDPE, low density
733 PE; PED4, perdeuterated polyethylene; IR, infrared; FTIR,
734 Fourier transform infrared; μ FTIR, FTIR microspectroscopy

735 REFERENCES

736 (1) Geyer, R.; Jambeck, J. R.; Law, K. L. Production, Use, and Fate
737 of All Plastics Ever Made. *Sci. Adv.* **2017**, *3* (7), e1700782
738 DOI: 10.1126/sciadv.1700782.
739 (2) Tokiwa, Y.; Calabia, B.; Ugwu, C.; Aiba, S. Biodegradability of
740 Plastics. *Int. J. Mol. Sci.* **2009**, *10* (9), 3722–3742.
741 (3) Yamada-Onodera, K.; Mukumoto, H.; Katsuyaya, Y.; Saiganji,
742 A.; Tani, Y. Degradation of Polyethylene by a Fungus, *Penicillium*
743 *Simplicissimum* YK. *Polym. Degrad. Stab.* **2001**, *72* (2), 323–327.
744 (4) Bonhomme, S.; Cuer, A.; Delort, A. M.; Lemaire, J.; Sancelme,
745 M.; Scott, G. Environmental Biodegradation of Polyethylene. *Polym.*
746 *Degrad. Stab.* **2003**, *81* (3), 441–452.
747 (5) Yoshida, S.; Hiraga, K.; Takehana, T.; Taniguchi, I.; Yamaji, H.;
748 Maeda, Y.; Toyohara, K.; Miyamoto, K.; Kimura, Y.; Oda, K. A
749 Bacterium That Degrades and Assimilates Poly(Ethylene Tereph-
750 thalate). *Science (Washington, DC, U. S.)* **2016**, *351* (6278), 1196–
751 1199.

(6) Restrepo-Flórez, J. M.; Bassi, A.; Thompson, M. R. Microbial
752 Degradation and Deterioration of Polyethylene - A Review. *Int.*
753 *Biodeterior. Biodegrad.* **2014**, *88* (March), 83–90.
754 (7) Yang, Y.; Yang, J.; Wu, W. M.; Zhao, J.; Song, Y.; Gao, L.; Yang,
755 R.; Jiang, L. Biodegradation and Mineralization of Polystyrene by
756 Plastic-Eating Mealworms: Part 2. Role of Gut Microorganisms.
757 *Environ. Sci. Technol.* **2015**, *49* (20), 12087–12093.
758 (8) Yang, Y.; Wang, J.; Xia, M. Biodegradation and Mineralization of
759 Polystyrene by Plastic-Eating Superworms *Zophobas Atratus*. *Sci.*
760 *Total Environ.* **2020**, *708*, 135233.
761 (9) Yang, S. S.; Wu, W. M.; Brandon, A. M.; Fan, H. Q.; Receveur, J.
762 P.; Li, Y.; Wang, Z. Y.; Fan, R.; McClellan, R. L.; Gao, S. H.; Ning, D.;
763 Phillips, D. H.; Peng, B. Y.; Wang, H.; Cai, S. Y.; Li, P.; Cai, W. W.;
764 Ding, L. Y.; Yang, J.; Zheng, M.; Ren, J.; Zhang, Y. L.; Gao, J.; Xing,
765 D.; Ren, N. Q.; Waymouth, R. M.; Zhou, J.; Tao, H. C.; Picard, C. J.;
766 Benbow, M. E.; Criddle, C. S. Ubiquity of Polystyrene Digestion and
767 Biodegradation within Yellow Mealworms, Larvae of *Tenebrio*
768 *Molitor* Linnaeus (Coleoptera: Tenebrionidae). *Chemosphere* **2018**,
769 *212*, 262–271.
770 (10) Peng, B. Y.; Su, Y.; Chen, Z.; Chen, J.; Zhou, X.; Benbow, M.
771 E.; Criddle, C. S.; Wu, W. M.; Zhang, Y. Biodegradation of
772 Polystyrene by Dark (*Tenebrio Obscurus*) and Yellow (*Tenebrio*
773 *Molitor*) Mealworms (Coleoptera: Tenebrionidae). *Environ. Sci.*
774 *Technol.* **2019**, *53* (9), 5256–5265.
775 (11) Bombelli, P.; Howe, C. J.; Bertocchini, F. Polyethylene Bio-
776 Degradation by Caterpillars of the Wax Moth *Galleria Mellonella*.
777 *Curr. Biol.* **2017**, *27* (8), R292–R293.
778 (12) Ren, L.; Men, L.; Zhang, Z.; Guan, F.; Tian, J.; Wang, B.;
779 Wang, J.; Zhang, Y.; Zhang, W. Biodegradation of Polyethylene by
780 *Enterobacter* Sp. D1 from the Guts of Wax Moth *Galleria Mellonella*.
781 *Int. J. Environ. Res. Public Health* **2019**, *16* (11), 1941.
782 (13) Kundungal, H.; Gangarapu, M.; Sarangapani, S.; Patchaiyappan,
783 A.; Devipriya, S. P. Efficient Biodegradation of Polyethylene (HDPE)
784 Waste by the Plastic-Eating Lesser Waxworm (*Achroia Grisella*).
785 *Environ. Sci. Pollut. Res.* **2019**, *26* (18), 18509–18519.
786 (14) Kong, H. G.; Kim, H. H.; Chung, J.; Jun, J. H.; Lee, S.; Kim, H.
787 M.; Jeon, S.; Park, S. G.; Bhak, J.; Ryu, C. M. The *Galleria Mellonella*
788 Hologenome Supports Microbiota-Independent Metabolism of Long-
789 Chain Hydrocarbon Beeswax. *Cell Rep.* **2019**, *26* (9), 2451–2464.e5.
790 (15) Kundungal, H.; Gangarapu, M.; Sarangapani, S.; Patchaiyappan,
791 A.; Devipriya, S. P. Role of Pretreatment and Evidence for the
792 Enhanced Biodegradation and Mineralization of Low-Density Poly-
793 ethylene Films by Greater Waxworm. *Environ. Technol.* **2021**, *42*, 717.
794 (16) Cassone, B. J.; Grove, H. C.; Elebute, O.; Villanueva, S. M. P.;
795 LeMoine, C. M. R. Role of the Intestinal Microbiome in Low-Density
796 Polyethylene Degradation by Caterpillar Larvae of the Greater Wax
797 Moth. *Proc. R. Soc. London, Ser. B* **2020**, *287* (1922), 20200112.
798 (17) Roy, D. N. On the Nutrition of Larvae of Bee-Wax Moth,
799 *Galleria Mellonella*. *J. Comp. Physiol., A* **1937**, *24* (5), 638–643.
800 (18) Lou, Y.; Ekaterina, P.; Yang, S. S.; Lu, B.; Liu, B.; Ren, N.;
801 Corvini, P. F. X.; Xing, D. Biodegradation of Polyethylene and
802 Polystyrene by Greater Wax Moth Larvae (*Galleria Mellonella* L.) and
803 the Effect of Co-Diet Supplementation on the Core Gut Microbiome.
804 *Environ. Sci. Technol.* **2020**, *54* (5), 2821–2831.
805 (19) Weber, C.; Pusch, S.; Opatz, T. Polyethylene Bio-Degradation
806 by Caterpillars? *Curr. Biol.* **2017**, *27*, R744–R745.
807 (20) Sandt, C.; Waeytens, J.; Deniset-Besseau, A.; Nielsen-Leroux,
808 C.; Réjasse, A. Use and Misuse of FTIR Spectroscopy for Studying
809 the Bio-Oxidation of Plastics. *Spectrochim. Acta, Part A* **2021**, *258*,
810 119841.
811 (21) Hagemann, H.; Snyder, R. G.; Peacock, A. J.; Mandelkern, L.
812 Quantitative Infrared Methods for the Measurement of Crystallinity
813 and Its Temperature Dependence: Polyethylene. *Macromolecules*
814 **1989**, *22* (9), 3600–3606.
815 (22) Poirier, S.; Rué, O.; Peguilhan, R.; Coeuret, G.; Zagorec, M.;
816 Champomier-Vergès, M. C.; Loux, V.; Chaillou, S. Deciphering Intra-
817 Species Bacterial Diversity of Meat and Seafood Spoilage Microbiota
818 Using GyrB Amplicon Sequencing: A Comparative Analysis with 16S
819

- 820 RDNA V3-V4 Amplicon Sequencing. *PLoS One* **2018**, *13* (9),
821 e0204629.
- 822 (23) Dumas, P.; Polack, F.; Lagarde, B.; Chubar, O.; Giorgetta, J. L.;
823 Lefrançois, S. Synchrotron Infrared Microscopy at the French
824 Synchrotron Facility SOLEIL. *Infrared Phys. Technol.* **2006**, *49* (1–
825 2), 152–160.
- 826 (24) Demšar, J.; Curk, T.; Erjavec, A.; Hočevar, T.; Milutinovič, M.;
827 Možina, M.; Polajnar, M.; Toplak, M.; Starič, A.; Stajdohar, M.;
828 Umek, L.; Zagar, L.; Zbontar, J.; Zitnik, M.; Zupan, B. Orange: Data
829 Mining Toolbox in Python. *J. Mach. Learn. Res.* **2013**, *14*, 2349–2353.
- 830 (25) Toplak, M.; Birarda, G.; Read, S.; Sandt, C.; Rosendahl, S. M.;
831 Vaccari, L.; Demšar, J.; Borondics, F. Infrared Orange: Connecting
832 Hyperspectral Data with Machine Learning. *Synchrotron Radiat. News*
833 **2017**, *30* (4), 40–45.
- 834 (26) Miller, L. M.; Dumas, P. From Structure to Cellular Mechanism
835 with Infrared Microspectroscopy. *Curr. Opin. Struct. Biol.* **2010**, *20*
836 (5), 649–656.
- 837 (27) Sandt, C.; Dionnet, Z.; Toplak, M.; Fernandez, E.; Brunetto, R.;
838 Borondics, F. Performance Comparison of Aperture-Less and
839 Confocal Infrared Microscopes. *J. Spectr. Imaging* **2019**, *8*, a8.
- 840 (28) Peng, C.; Kaščáková, S.; Chiappini, F.; Olaya, N.; Sandt, C.;
841 Yousef, I.; Samuel, D.; Dumas, P.; Guettier, C.; Le Naour, F.
842 Discrimination of Cirrhotic Nodules, Dysplastic Lesions and
843 Hepatocellular Carcinoma by Their Vibrational Signature. *J. Transl.*
844 *Med.* **2016**, *14* (1), 9.
- 845 (29) Kselíková, V.; Vitová, M.; Bišová, K. Deuterium and Its Impact
846 on Living Organisms. *Folia Microbiol. (Dordrecht, Neth.)* **2019**, *64*,
847 673.
- 848 (30) Marshall, C.; Javaux, E.; Knoll, a; Walter, M. Combined Micro-
849 Fourier Transform Infrared (FTIR) Spectroscopy and Micro-Raman
850 Spectroscopy of Proterozoic Acritarchs: A New Approach to
851 Palaeobiology. *Precambrian Res.* **2005**, *138* (3–4), 208–224.
- 852 (31) Billen, P.; Khalifa, L.; Van Gerven, F.; Tavernier, S.; Spatari, S.
853 Technological Application Potential of Polyethylene and Polystyrene
854 Biodegradation by Macro-Organisms Such as Mealworms and Wax
855 Moth Larvae. *Sci. Total Environ.* **2020**, *735*, 139521.
- 856 (32) Lemoine, C. M. R.; Grove, H. C.; Smith, C. M.; Cassone, B. J.
857 A Very Hungry Caterpillar: Polyethylene Metabolism and Lipid
858 Homeostasis in Larvae of the Greater Wax Moth (*Galleria*
859 *Mellonella*). *Environ. Sci. Technol.* **2020**, *54* (22), 14706–14715.
- 860 (33) Yang, Y.; Yang, J.; Wu, W. M.; Zhao, J.; Song, Y.; Gao, L.; Yang,
861 R.; Jiang, L. Biodegradation and Mineralization of Polystyrene by
862 Plastic-Eating Mealworms: Part I. Chemical and Physical Character-
863 ization and Isotopic Tests. *Environ. Sci. Technol.* **2015**, *49* (20),
864 12080–12086.
- 865 (34) Zhang, J.; Gao, D.; Li, Q.; Zhao, Y.; Li, L.; Lin, H.; Bi, Q.;
866 Zhao, Y. Biodegradation of Polyethylene Microplastic Particles by the
867 Fungus *Aspergillus Flavus* from the Guts of Wax Moth *Galleria*
868 *Mellonella*. *Sci. Total Environ.* **2020**, *704*, 135931.
- 869 (35) Yang, J.; Yang, Y.; Wu, W. M.; Zhao, J.; Jiang, L. Evidence of
870 Polyethylene Biodegradation by Bacterial Strains from the Guts of
871 Plastic-Eating Waxworms. *Environ. Sci. Technol.* **2014**, *48* (23),
872 13776–13784.
- 873 (36) Matjašič, T.; Simčič, T.; Medvešček, N.; Bajt, O.; Dreo, T.;
874 Mori, N. Critical Evaluation of Biodegradation Studies on Synthetic
875 Plastics through a Systematic Literature Review. *Sci. Total Environ.*
876 **2021**, *752*, 141959.